

Increase in the Specific Surface Area of Budesonide during Storage Postmicronization

Vidya Joshi,^{1,3} Sarvajna Dwivedi,² and Gary H. Ward¹

Received June 28, 2001; accepted September 27, 2001

Purpose. To evaluate an anomalous increase in the specific surface area of budesonide during storage postmicronization.

Methods. Budesonide was micronized using a conventional air-jet mill. Surface areas and total pore volumes were measured using nitrogen sorption. Porosity was measured using mercury intrusion porosimetry. Particle size was measured using laser diffraction.

Results. Budesonide exhibited a surface area increase of $22 \pm 2\%$ when stored at 25°C following micronization. The rate of surface area increase was lower at 20°C, suggesting a temperature-dependent stress relaxation mechanism for the micronized particles. The increase in surface area was accompanied by: (a) an increase in total pore volume; (b) a shift of the pore size distribution to smaller pore sizes; (c) a decrease in size of particles above $\sim 1 \mu\text{m}$; and (d) an increase in rugosity/surface roughness.

Conclusions. Freshly micronized budesonide exhibited an unusual and significant postmicronization increase in specific surface area upon storage under ambient conditions. Postmicronization stress-relief by intraparticle crack formation, crack propagation with time, and particle fracture seems to be the primary mechanism behind this surface area increase.

KEY WORDS: budesonide; cracks; increase; micronization; storage; surface area.

INTRODUCTION

Dry powder inhalation aerosols (DPIs) have been developed for pulmonary delivery of anti-inflammatory steroids and antiasthmatic agents as an alternative to pressurized metered-dose inhalation aerosols. It is generally accepted that the drug used in dry powder inhalers (1) should have an aerodynamic diameter between 1 and 6 μm for deep lung penetration (2,3). Often, this requires significant size reduction of the active drug present in such aerosols.

Grinding with fluid energy is a widely utilized method of breaking solids into fine particles to obtain the desired aerodynamic diameter (4). In a fluid energy mill, the particles are suspended in high-velocity jet streams of air, and the size reduction is caused by the high-speed particle-particle or particle-surface impact (4). Micronized particles show higher particle cohesiveness and higher particle-bonding index compared to materials milled by other processes (5). Hence, they

may show an increased tendency to agglomerate, leading to a reduction in surface area when stored postmicronization. Such changes may adversely affect, for example, the dispersibility of a DPI formulation. In other cases, the surface energy of the powder may be altered as a consequence of fluid-energy milling, which can disrupt the orientation of molecules on the surface (6). Consequently, localized crystalline disorder in the form of amorphous regions may be introduced onto particle surfaces (7). Amorphous regions created by the milling process may also have a significant impact on the dispersibility of aerosol formulations (8,9). The amorphous regions can further induce the formation of solid bridges between particles during storage or exposure to high temperature/humidity conditions (10). Such processes can also cause an irreversible increase in the particle size and/or reduction in the surface area of micronized powders.

Any processing or storage condition that can cause a change in the particle size or surface area of micronized drug used in a DPI formulation should be monitored and controlled to ensure formulation consistency during manufacturing and storage. In an attempt to understand whether such changes could occur with micronized steroids, postmicronization changes in budesonide were characterized. Contrary to expectations, micronized budesonide showed an 'increase' in surface area with time at ambient storage conditions. Micromeritic and solid state properties of micronized budesonide were investigated further to understand the mechanism behind such anomalous change.

MATERIALS AND METHODS

Micronization of Budesonide

One lot of budesonide was milled with a 2" Micron Master Jet Pulverizer jet mill (The Jet Pulverizer Company, Moorestown, NJ) using nitrogen as the milling fluid. The orientation of the mill was clockwise. The milling nozzle pressure was set between 35 and 50 psi, and the injection nozzle pressure at 100 psi, to obtain particles in the respirable range (99% particles $< 10 \mu\text{m}$; median particle size, $\sim 1\text{--}6 \mu\text{m}$). The drug was fed manually into the mill at a feed rate of $\sim 5 \text{g/min}$. Micronization was carried out at two temperatures (20°C and 25°C) to understand the effect of variations in ambient temperature conditions on the anomalous surface area increase. Each lot was stored at the same temperature at which it was milled. For instance, lot A was milled at 20°C, following which it was stored at 20°C in a closed container.

Surface Area and Total Pore Volume Measurement

Specific surface area measurements were made using the AUTOSORB 3B multi-station gas sorption surface area analyzer (Quantachrome Corp., Boynton Beach, FL) using nitrogen as the adsorbate and applying the Brunauer-Emmett-Teller (BET) equation, as described elsewhere (11). In addition, the total pore volume was calculated at the highest programmed relative partial pressure point ($P/P_o = 0.995$) by assuming that the pores are filled with liquid adsorbate at such high partial pressures. Surface area measurements were carried out in triplicate for each lot and at each time point. Approximately 0.2 g micronized budesonide was placed in each sample cell, and the outgassing process was conducted

¹ Dura Pharmaceuticals, 7473 Lusk Boulevard, San Diego, California 92121.

² Advanced Inhalation Research, Inc., 840 Memorial Drive, Cambridge, Massachusetts 02139.

³ To whom correspondence should be addressed at 16 Leonard Street Waltham Massachusetts 02451. (e-mail: vidya_joshi@hotmail.com)

ABBREVIATIONS: BET, Brunauer-Emmett-Teller; DPI, dry powder inhalation aerosol.

using a vacuum at ambient temperature over 6 h. For each sample, a 21-point isotherm (10-point adsorption, 10-point desorption, with a common adsorption/desorption point at the transition point) was collected, followed by a 5-point BET surface area analysis.

Pore Size Distributions by Mercury Intrusion Porosimetry

Pore size distributions were measured by mercury intrusion porosimetry using the POREMASTER GT mercury porosimeter (Quantachrome Corp.). The experimental procedure consisted of loading a sample (~0.2 g) into a low-pressure penetrometer cell. The cell was evacuated to extremely low pressures to remove contaminants. The intrusion was monitored via a change in capacitance of the mercury column in the penetrometer cell from 0.007 to 0.34 MPa in the low-pressure chamber and 0.14 to 8.0 MPa in the high-pressure chamber.

Particle Size Measurements by Laser Diffraction

Particle size distribution of micronized budesonide as a function of time was measured on a Sympatec HELOS 3.3® laser diffraction apparatus (Sympatec GmbH, Glausthal Zellenfeld, Germany). This instrument is equipped with a RODOS powder disperser and a R2 lens, which allows measurement of narrow particle size distributions in the range of 0.4–87.5 μm . It measures the powder particle size distributions by laser diffraction when the powder is dispersed in air as a stream of gas-solid aerosol. The measurement parameters were as follows: (a) a primary dispersion pressure of 4 bar, which was found to be adequate to disperse any agglomerates of the micronized drug particles, and thus allowed measurement of primary drug particle size; and (b) a vibratory feed rate of 50% on the RODOS disperser for consistent feeding of the powder samples into the air stream. The consistency of HELOS's performance over the analysis period was verified by periodically testing a silicon carbide powder (SiC1200'93, Sympatec GmbH) standard.

RESULTS AND DISCUSSION

Surface Area by Nitrogen Adsorption

Four lots of micronized budesonide were generated from a single-parent lot of nonmicronized budesonide using the micronization parameters described before. Figure 1 shows the BET surface area-time profiles of each of the four lots, A–D, following micronization ($n = 3$; error bars = 1 SD).

To minimize sampling-related bias, the surface area of micronized budesonide was monitored in two ways. The first technique involved the withdrawal of fresh samples at each timepoint from the bulk container, whereas the second involved monitoring the surface area of the same sample stored in the sample cell as a function of time. Surface areas of lots A, B, and C were measured using the former technique, and that of lot D using the latter. The significant increase in surface area exhibited by all four lots confirms that the anomalous surface area increase is not an artifact related to powder handling.

To understand the effect of variations in ambient temperature, lot A was milled and subsequently stored at 20°C and lots B–D were milled and subsequently stored at 25°C.

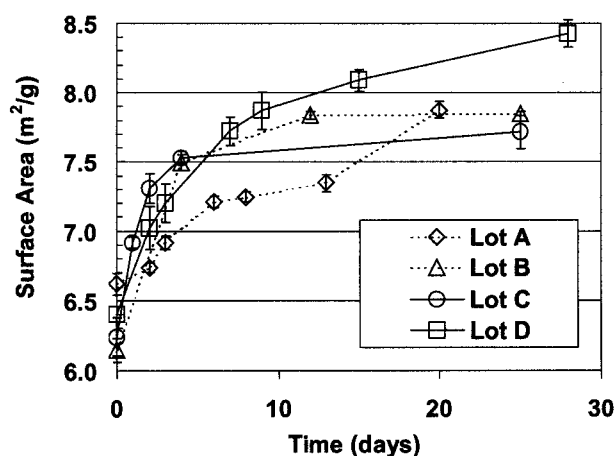


Fig. 1. BET surface areas of four lots of micronized budesonide as a function of time.

The initial surface area of lot A was $6.6 \pm 0.1 \text{ m}^2/\text{g}$, whereas the average initial surface area of lots B–D was $\sim 6.2 \text{ m}^2/\text{g}$. The surface area at the end of the study was $7.9 \pm 0.1 \text{ m}^2/\text{g}$ for lot A and $\sim 8.0 \text{ m}^2/\text{g}$ for lots B–D. Lots B–D (stored at 25°C) not only exhibited a larger average increase in surface area but also a greater rate of surface area increase over the first week postmicronization when compared to lot A (see Fig. 1). These observations suggest an impact of temperature on the extent and potential mechanism of surface area increase.

Physical and Chemical Characterization of Micronized Budesonide during the Time Scale of the Experiment

The physical form of the nonmicronized material was found to be anhydrous budesonide as determined by thermal analysis ($\text{mp} \sim 260^\circ\text{C}$) and X-ray powder diffraction. There was no change in physical form upon micronization. However, micronization induced the formation of a finite amount of amorphous budesonide ($\sim 5\%$) as measured by organic vapor sorption (12). This amorphous material was undetectable by water vapor sorption methods, and the amorphous-to-crystalline phase transition was not mediated by water during the time scale of this experiment. However, when monitoring the amorphous content by organic vapor sorption (12) over the same time scale as the surface area increase, no significant change in amorphous content of micronized budesonide was observed. Furthermore, micronized material stored under ambient conditions for one month was found to remain physically stable (no polymorphic transitions) as confirmed by thermal analysis and X-ray powder diffraction. The chemical impurity profile of the lot used in this study was representative of the profile observed for other lots of crystalline budesonide. There was no change in the impurity profile throughout the time scale of this study.

Mechanism of Surface Area Increase

There have been very few published examples of such anomalous surface area increases in pharmaceutical solids during storage. Zimeldine dihydrochloride tetrahydrate is one such example, which exhibits a surface area increase upon aging (13). This compound has four highly mobile water molecules in its unit cell, which change with time. The presence of these water molecules results in mechanical stresses

within the aging unit cell, leading to a cracking of the crystals, which in turn causes a surface area increase. At higher temperatures, the cracking process was more rapid, suggesting the catalytic role of temperature in crack advancement and subsequent surface area increase. This observation is consistent with the effect of temperature observed in the present study.

The following hypothesis is proposed to explain the anomalous increase in surface area of micronized budesonide. Crystal fracture may occur as a result of crack advancement under the influence of externally imposed and/or internally generated stresses (14). Zimeldine dihydrochloride tetrahydrate is a good example of the latter case, where internally generated stresses due to the labile water molecules resulted in cracking and corresponding surface enlargement during aging. Micronized budesonide would be a good example to illustrate the former case, where surface enlargement is a consequence of internal 'residual' stresses left behind from the external stresses imposed during micronization.

Micronization is an energy-intensive operation that applies significant external stress to particles, and introduces localized regions of high energy such as cracks, point defects, and dislocations (15). Some of the micronized particles may have formed cracks during micronization, or new cracks may emanate from these defects due to their high residual stresses. This type of fracture may be classified as a mode I fracture (14). A mode I fracture typically occurs at low stress levels at splits or cracks, increasing the internal strain and producing a stress concentration at the tip of the crack (14,16). Therefore, at a given stress level, cracks may propagate, resulting in secondary cracks if they are above a certain critical size. If the cracks are large, then their propagation may be severe, causing particle fracture. The combined processes of crack propagation, new crack formation, and particle fracture will expose new surfaces, and hence cause an increase in the specific surface area of the powder postmicronization. This hypothesis is schematically represented in Fig. 2.

For micronized budesonide, this hypothesis was tested by performing the following analyses: (a) measurement of the total pore (or crack or void) volume using nitrogen sorption to determine if there is a change in pore volume with time, supporting the formation of new cracks; (b) measurement of the pore size distributions using mercury intrusion porosimetry to estimate any changes in the pore size during storage; (c) measurement of the particle size using laser diffraction to confirm if any change in the particle size distribution occurs as a result of particle fracture; and (d) estimation of the rugosity of micronized particles to understand the contribution of surface roughness in surface area changes.

Total Pore Volume by Nitrogen Sorption

Figure 3 shows the change in the total pore volumes and specific surface areas of the four lots of micronized budesonide as a function of time. There is an increase in total pore volume with time for all four lots. Regression analysis of the pooled pore volumes for the four lots vs. their corresponding specific surface area values (Fig. 4) showed a statistically significant correlation between the two parameters ($R^2 = 0.73$). An increase in pore volume supports the first step of the hypothesis (Fig. 2) that micronized particles could undergo stress relaxation. This leads to the formation of new pores or

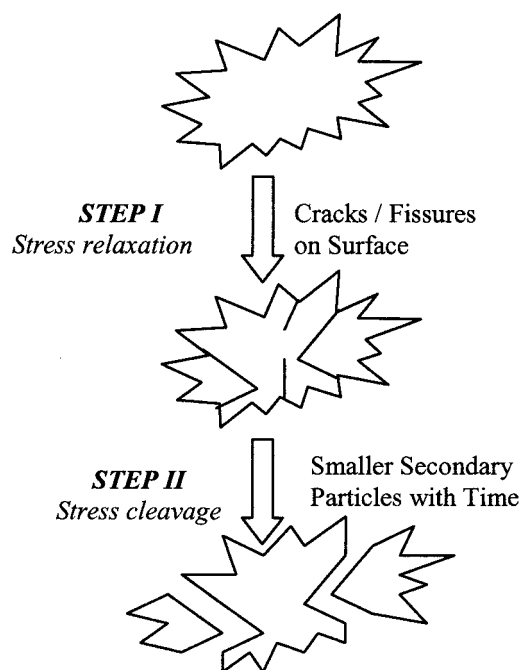


Fig. 2. Proposed hypothesis to explain the postmicronization increase in surface area of micronized budesonide.

cracks, the growth of previously existing pores or cracks, or a combination of both, resulting in an associated increase in porosity. This exposes additional surface, which in turn is reflected in a greater volume of nitrogen adsorption and a subsequent increase in specific surface area.

Pore Size Distribution by Mercury Intrusion Porosimetry

The increase in total pore volume as measured by nitrogen adsorption was further explored by mercury intrusion porosimetry. Figure 5 shows the log differential intrusion curves, $dV/d(\log d)$ for micronized budesonide particles (lot A) at different time points. The peaks of the four curves correspond to the measured pore diameters at the different time points. The distribution of pore diameters shifts to smaller size as a function of time, suggesting the formation of new and smaller pores. This is consistent with the increase in total pore volume, as seen in Fig. 3. The shift in pore distributions to smaller pore size also supports the hypothesis of secondary pore formation during storage due to the propagation of primary cracks formed during micronization. In the case of particles where crack propagation is severe, the particles could also fracture. This was explored further by laser diffraction analysis of the micronized particles with time during storage.

Particle Size by Laser Diffraction

Figure 6 is a plot of the volume median diameter ($\times 50$), 90% undersize ($\times 90$), and 99% undersize ($\times 99$) of micronized budesonide (lot A) with storage time. A significant decrease in $\times 50$ was observed, which was consistent with the increase in surface area. Similar trends were seen with 90% undersize ($\times 90$) and 99% undersize ($\times 99$) cutoffs. These observations suggest that the micronized primary particles fracture at the cleavage planes created by the cracks to cause an effective

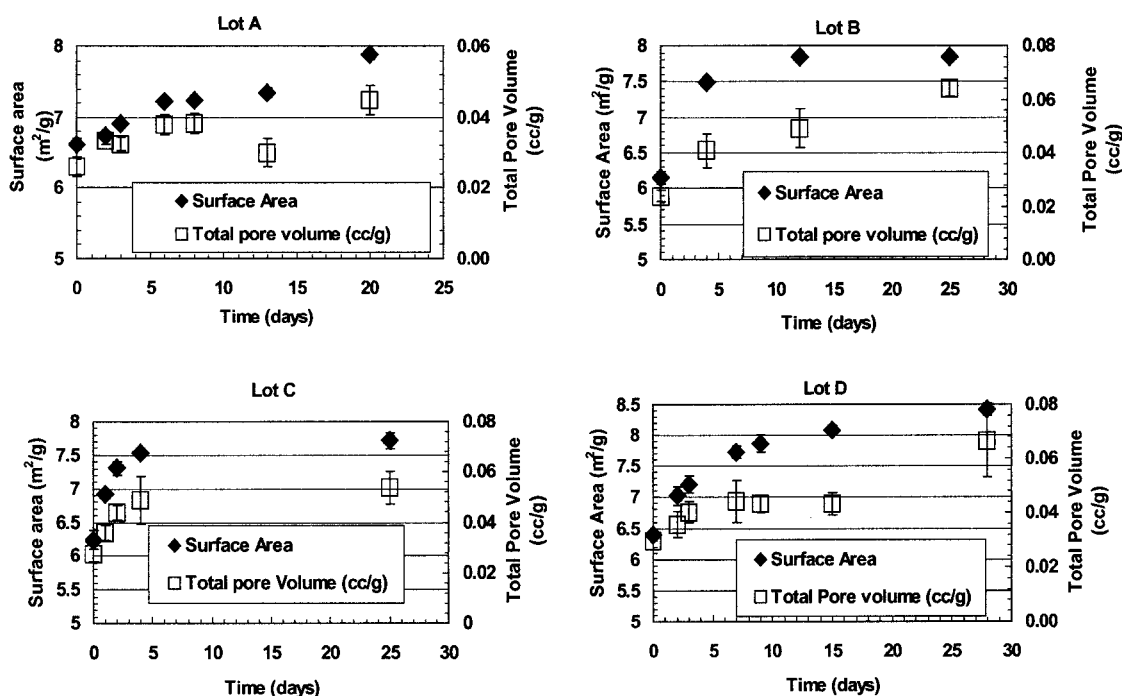


Fig. 3. Total pore volumes (measured by nitrogen sorption) overlaid with BET surface areas of lots A–D of micronized budesonide.

decrease in the overall particle size of the micronized budesonide.

Full particle size distributions (7) of micronized budesonide (lot A) measured during storage postmicronization show a progressive decrease in particle size. However, in the submicron particle size range, there was a crossover of the particle size distributions between 0 and 21 days. This may be due to two competing processes occurring concurrently, where the first process causes the gradual reduction in the number of submicron particles (as they agglomerate to form larger particles) and the second process involves crack propagation and fracture of larger particles (resulting in an increase in the percentage of particles $>1 \mu\text{m}$). This hypothesis is confirmed by the trends in the $\times 50$, $\times 90$, and $\times 99$ cutoffs (Fig. 6), and by the shift in particle size distribution above $1 \mu\text{m}$ to lower particle sizes (Fig. 7). The decrease in size of particles

above $1 \mu\text{m}$ supports the second step of the hypothesis (Fig. 2) that micronized particles undergo stress cleavage, which in turn would result in smaller secondary particles and a subsequent decrease in overall particle size of the micronized particles after storage. The net effect of the reduction in particle size distribution would be an increase in the specific surface area. The surface area increase due to particle size changes could be augmented by the change in surface area due to an increase in surface roughness, which was explored further by rugosity estimation.

Estimation of Rugosity

Rugosity is a qualitative measure of the macroscopic shape and surface textures of materials. An estimate of rugosity (17) can be derived from the following formula:

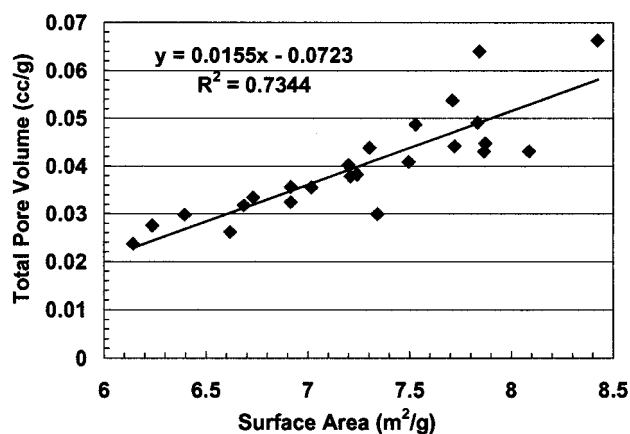


Fig. 4. Regression analysis of pooled pore volumes of lots A–D of micronized budesonide vs. their corresponding surface area values.

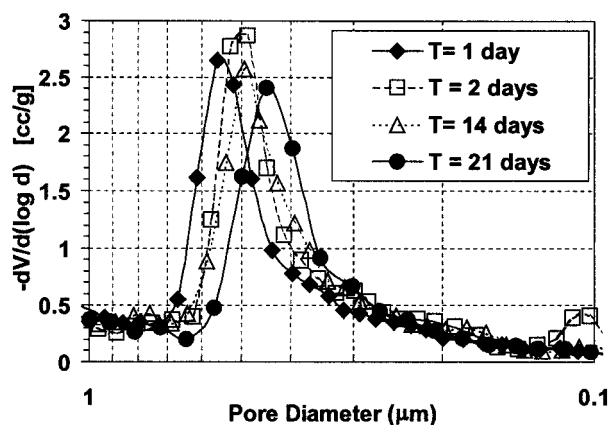


Fig. 5. A plot of pore size distributions of micronized budesonide measured using mercury intrusion porosimetry at different time points.

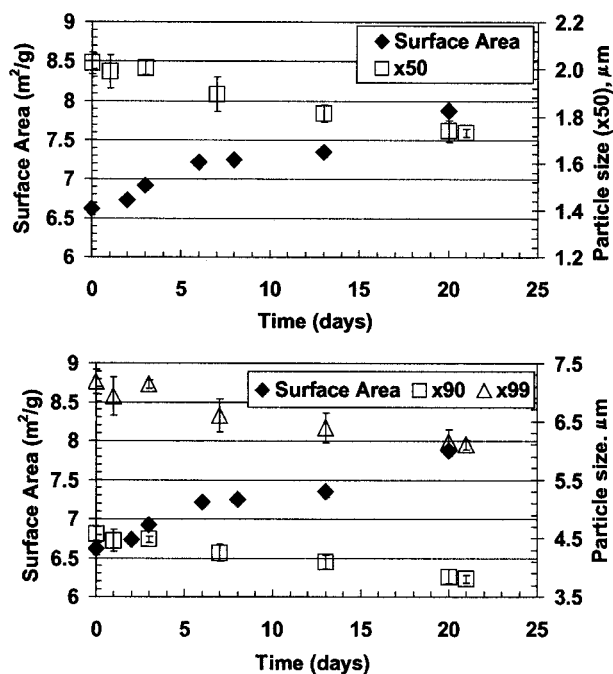


Fig. 6. Surface area of lot A of micronized budesonide overlaid with volume median diameter, $\times 50$ (top), and particle size expressed as cumulative percent undersize, $\times 90$ and $\times 99$ (bottom).

$$R_a = \frac{\text{Measured BET Surface Area}}{\text{Calculated Surface Area from Particle Size Measurements}} \quad (1)$$

Particle size measurements determined by laser diffraction assumes that particles are (a) spheres and (b) have smooth surfaces. The surface area calculated from such particle size measurements does not account for surface roughness or the shape of particles. The surface area calculated from gas sorption accounts for cracks, crevices, or pores within the structure of particles. Therefore, the ratio of the surface areas

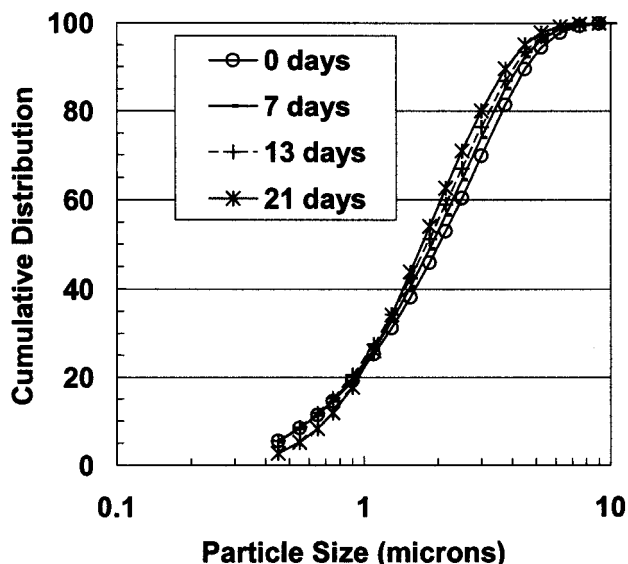


Fig. 7. Cumulative particle size distributions of aged micronized budesonide at different time points.

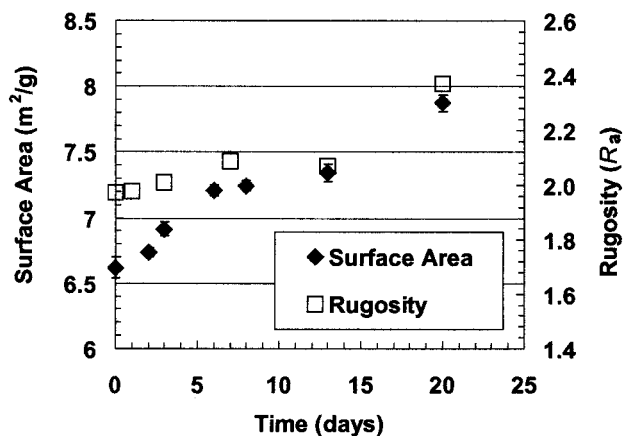


Fig. 8. A plot of the R_a overlaid with surface area of lot A of micronized budesonide with time.

calculated by these two methods gives an estimate of the surface area that can be attributed to surface irregularities, provided there are no gross changes in the shape of particles during storage.

It should, however, be noted that rugosity comparisons might not be able to distinguish between surface smoothness or textures of two particles, if they differ substantially in macroscopic shape (18). The overall macroscopic shape of micronized budesonide particles did not change substantially upon aging (confirmed from electron micrographs taken before and after the surface area increase). Hence, the above calculation of rugosity may be used at least qualitatively to estimate changes in surface roughness of micronized budesonide over time.

Figure 8 is a plot of the rugosity estimates (R_a) of the micronized budesonide particles during storage. An increase in rugosity from ~ 2.0 to 2.4 was observed at the end of 3 weeks, suggesting an increase in defects or crystal abnormalities, which would contribute to the increase in specific surface area during storage postmicronization.

CONCLUSIONS

Micronized budesonide exhibits a significant postmicronization increase in specific surface area upon storage under ambient conditions. The surface area increase was accelerated when the storage temperature was increased, suggesting a temperature-dependent stress relaxation mechanism for the micronized particles. The increase in surface area was accompanied by: (a) an increase in total pore volume; (b) a shift of the pore size distribution to smaller pore sizes; (c) a decrease in size of particles above $\sim 1 \mu\text{m}$; and (d) an increase in rugosity/surface roughness. These observations support the hypothesis that for some organic solids, micronized particles may have residual stresses stored in the form of cracks and other defects, which may lead to the formation of additional cracks or defects during storage by a stress relief process. The cracks may propagate to form larger cracks, some of which may eventually cause particle fracture to form new secondary particles. It is possible that the properties of solid dosage forms prepared with fresh or stored drug may be different, particularly if their performance exhibits a strong dependence on particle size or other surface properties. It is important, therefore, to study the micromeritic properties of pharmaceu-

tical organic solids carefully when they are subjected to high-energy particle size reduction processes.

REFERENCES

1. D. Ganderton. The generation of respirable cloud from coarse powder aggregates. *J. Biopharm. Sci.* **3**:101–105 (1992).
2. S. P. Newman and S. W. Clarke. Therapeutic aerosols: I. Physical and practical considerations. *Thorax* **38**:881–886 (1983).
3. I. Gonda. Aerosols for delivery of therapeutic and diagnostic agents to the respiratory tract. *CRC Crit. Rev. Ther. Drug Carrier Syst.* **6**:273 (1990).
4. L. G. Austin and O. Trass. Size reduction of solids: crushing and grinding equipment. In M. E. Fayed, L. Otten (eds.), *Handbook of Powder Science and Technology*, Chapman & Hall, New York, 1997 pp. 586–634.
5. M. O. Omelczuk, C. C. Wang, and D. G. Pope. Influence of micronization on the compaction properties of an investigational drug using tableting index analysis. *Eur. J. Pharm. Biopharm.* **43**:95–100 (1997).
6. G. Buckton, A. Choularton, A. E. Beezer, and S. M. Chatham. The effect of comminution technique on the surface energy of a powder. *Int. J. Pharm.* **47**:121–128 (1988).
7. A. A. Elamin, T. Sebhatu, and C. Ahlneck. The use of amorphous model substances to study mechanically activated materials in the solid state. *Int. J. Pharm.* **119**:25–36 (1995).
8. R. O. Williams III, J. Brown, and J. Liu. Influence of micronization method on the performance of a suspension triamcinolone acetonide pressurized metered dose inhaler formulation. *Pharm. Dev. Technol.* **4**:167–179 (1999).
9. E. M. Phillips and P. R. Byron. Surfactant promoted crystal growth of micronized methylprednisolone in trichloromonofluoromethane. *Int. J. Pharm.* **110**:9–19 (1994).
10. G. H. Ward and R. K. Schultz. Process-induced crystallinity changes in albuterol sulfate and its effect on powder physical stability. *Pharm. Res.* **12**:773–779 (1995).
11. S. Brunauer, P. H. Emmett, and E. Teller. Adsorption of gases in multimolecular layers. *J. Am. Chem. Soc.* **60**:309–319 (1938).
12. V. Joshi, R. K. Cavatur, V. K. Cheruvallath, S. K. Dwivedi, and G. H. Ward. Anomalous organic vapor sorption by micronized budesonide at constant vapor pressure and temperature. *AAPS Pharm. Sci.* (Indianapolis). **4**:S3625 (2000).
13. H. Nyquist and T. Wadsten. Changes in surface area of zimeidine dihydrochloride hydrate on storage. *Acta Pharm. Suec.* **21**:235–244 (1984).
14. T. H. Courtney. *Mechanical Behavior of Materials*, McGraw-Hill Series in Mechanical Science and Engineering, McGraw-Hill Publishing Company, New York, 1990.
15. G. Mestl, B. Herzog, R. Schogl, and H. Knozinger. Mechanically activated Mo O₃ 1: particle size, crystallinity, and morphology. *Langmuir* **11**:3027–3034 (1995).
16. L. Hixon, H. Prem, M. Prior, and J. Van Cleef. *Fundamentals of Powder Technology: Focus on Size Reduction*, Hosokawa Micron International Inc. 1991, Summit, New Jersey.
17. J. T. Carstensen. *Solid Pharmaceutics: Mechanical Properties and Rate Phenomena*, Academic Press, London, England. 1980.
18. X. M. Zeng, G. P. Martin, C. Marriott, and J. Pritchard. The influence of carrier morphology on drug delivery by dry powder inhalers. *Int. J. Pharm.* **200**:93–106 (2000).